Transferability of Mie n-6 force fields for predicting liquid shear viscosity at saturation and elevated pressures

Richard A. Messerly

Thermodynamics Research Center, National Institute of Standards and Technology, Boulder, Colorado, 80305

Michelle C. Anderson, S. Mostafa Razavi, J. Richard Elliott

Abstract

Keywords:

Thermophysical Properties, Molecular Simulation

Key points

Mie and TAMie potentials are much better at saturation viscosities, despite not being fit directly to them Viscosity density curve is much harder to reproduce Viscosity pressure is adequately predicted with Potoff and TAMie Branched alkanes have slightly worse performance

Propane is accurate to nearly 1 GPa Butane agrees more closely with newer REFPROP correlation C12 has similar results for Potoff and TraPPE?

Entropy scaling for isooctane?

Wrong torsional parameters for some isocompounds?

Outline

1. Introduction

1. Viscosity is an important property for designing chemical systems
2. Viscosity data typically do not cover the entire range of $P\rho T$ of interest

Email address: richard.messerly@nist.gov (Richard A. Messerly)

3. Prediction methods are typically quite poor for viscosity
4. Molecular simulation is an attractive alternative, but two main challenges
   (a) Difficulty of obtaining reproducible results from simulation
   (b) Unreliable force fields
5. This manuscript applies the recent Best Practices to improve reproducibility such that it is possible to elucidate the difference in force fields
6. Previous studies have suggested that UA models may be inadequate, while Gordon showed that a Mie potential could accomplish both VLE and viscosity
7. This study tests whether the modern Mie potentials that are optimized for saturation thermodynamic properties are transferable to transport properties, e.g. shear viscosity

2. Methods

3. Molecular Dynamics

3.1. Force field

A united-atom (UA) or anisotropic-united-atom (AUA) representation is used for each compound studied. UA models assume that the UA interaction site is that of the carbon atom, while AUA models assume that the AUA interaction site is shifted away from the carbon atom and towards the hydrogen atom(s). Note that TraPPE and Potoff are UA force fields while TraPPE-2, AUA4, and TAMie are AUA force fields.

The UA and AUA groups required for normal and branched alkanes are sp^3 hybridized CH_3, CH_2, CH, and C sites. For most literature models, a single (transferable) parameter set is assigned for each interaction site. However, two exceptions exist for the force fields studied. First, TAMie implements a different set of CH_3 parameters for ethane. Second, Potoff reports a "generalized" and "short/long" (S/L) CH and C parameter set. The Potoff "generalized" CH and C parameter set is an attempt at a completely transferable set. However, since the "generalized" parameters performed poorly for some compounds, the S/L parameter set was proposed, where the "short" and "long" parameters are implemented when the number of carbons in the backbone is ≤ 4 and > 4, respectively.

A fixed bond-length is used for each bond between UA or AUA sites. Although TAMie is an AUA force field, only the terminal CH_3 sites have a displacement in the interaction site. For example, Figure 1 depicts both the UA and AUA representations of isooctane when only terminal CH_3 interaction sites are shifted from the carbon center. This convention is much simpler to implement than other AUA approaches (such as AUA4) where non-terminal (i.e. CH_2 and CH) interaction sites also have a displacement distance. For this reason, we do not attempt to simulate the AUA4 force field for any compounds containing CH_2 and CH interaction sites. For the compounds and force fields simulated, the anisotropic shift in a terminal interaction site (i.e. CH_3) is treated simply as a longer effective bond-length (see Table 1). The bond-length for all non-terminal sites is 0.154 nm, except for the Errington Exp-6 force field which uses 0.1535 nm for CH_2-CH_2 bonds.

Figure 1: AUA force fields have the same complexity as UA force fields if only the terminal (CH_3) sites have an anisotropic displacement, i.e. a longer effective bond-length. Note that the AUA4 representation of isooctane requires a more complicated shifting of CH_2 and CH sites than that depicted here.

The angle and dihedral energies are computed using the same functional forms for each force field. Angular bending interactions are evaluated using a harmonic potential:

$$u^{\text{bend}} = \frac{k_\theta}{2}\left(\theta - \theta_0\right)^2 \tag{1}$$

where u^{bend} is the bending energy, θ is the instantaneous bond angle, θ_0 is the equilibrium

Table 1: Effective bond-lengths in units of nm for terminal (CH_3) UA or AUA interaction sites. Empty table entries for TraPPE-2 denote that the force field does not contain the corresponding interaction site type. Empty table entries in AUA4 arise because this force field uses a more complicated construction than the simple effective bond-length approach. Specifically, AUA4 requires CH_2 and CH interaction sites that are not along the C-C bond axis.

Bond	TraPPE, Potoff	TAMie	AUA4	TraPPE-2
CH_3-CH_3	0.154	0.194	0.1967	0.230
CH_3-CH_2	0.154	0.174	–	–
CH_3-CH	0.154	0.174	–	–
CH_3-C	0.154	0.174	0.1751	–

bond angle, and k_θ is the harmonic force constant which is equal to 62500 K/rad^2 for all bonding angles. Dihedral torsional interactions are determined using a cosine series:

$$u^{\text{tors}} = c_0 + c_1[1 + \cos\phi] + c_2[1 - \cos 2\phi] + c_3[1 + \cos 3\phi] \tag{2}$$

where u^{tors} is the torsional energy, ϕ is the dihedral angle and c_i are the Fourier constants. The equilibrium bond angles and torsional parameters are found in Tables 2-3, respectively. Note that the Errington c_i values [**?**] for CH_x-CH_2-CH_2-CH_y are a factor of two less than those reported in Table 3.

Table 2: Equilibrium bond angles (θ_0). x and y are values between 0-3.

Bending sites	θ_0 (degrees)
CH_x-CH_2-CH_y	114.0
CH_x-CH-CH_y	112.0
CH_x-C-CH_y	109.5

Non-bonded interaction energies and forces between sites located in two different molecules or separated by more than three bonds are calculated using a Mie λ-6 potential (of which

Table 3: Fourier constants (c_i) in units of K. x and y are values between 0-3.

Torsion sites	c_0	c_1	c_2	c_3
CH_x-CH_2-CH_2-CH_y	0.0	355.03	-68.19	791.32
CH_x-CH_2-CH-CH_y	-251.06	428.73	-111.85	441.27
CH_x-CH_2-C-CH_y	0.0	0.0	0.0	461.29
CH_x-CH-CH-CH_y	-251.06	428.73	-111.85	441.27

the Lennard-Jones, LJ, 12-6 is a subclass), Equation **??**. The non-bonded Mie λ-6 force field parameters for TraPPE, TraPPE-2, Potoff, AUA4, and TAMie are provided in Table 4.

Table 4: Non-bonded (intermolecular) parameters for TraPPE [**?** **?**] (and TraPPE-2 [**?**]), Potoff [**?** **?**], AUA4 [**?** **?**], and TAMie [**?** **?**] force fields. The "short/long" Potoff CH and C parameters are included in parentheses. The ethane specific parameters for TAMie are included in parentheses.

	TraPPE (TraPPE-2)			Potoff (S/L)		
United-atom	ϵ (K)	σ (nm)	λ	ϵ (K)	σ (nm)	λ
CH_3	98 (134.5)	0.375 (0.352)	12	121.25	0.3783	16
CH_2	46	0.395	12	61	0.399	16
CH	10	0.468	12	15 (15/14)	0.46 (0.47/0.47)	16
C	0.5	0.640	12	1.2 (1.45/1.2)	0.61 (0.61/0.62)	16
	AUA4			TAMie		
CH_3	120.15	0.3607	12	136.318 (130.780)	0.36034 (0.36463)	14
CH_2	86.29	0.3461	12	52.9133	0.40400	14
CH	50.98	0.3363	12	14.5392	0.43656	14
C	15.04	0.244	12	–	–	–

Non-bonded interactions between two different site types (i.e. cross-interactions) are determined using Lorentz-Berthelot combining rules [**?**] for ϵ and σ, respectively, and an

arithmetic mean for the repulsive exponent λ (as recommended in Reference **?**):

$$\epsilon_{ij} = \sqrt{\epsilon_{ii}\epsilon_{jj}} \tag{3}$$

$$\sigma_{ij} = \frac{\sigma_{ii} + \sigma_{jj}}{2} \tag{4}$$

$$\lambda_{ij} = \frac{\lambda_{ii} + \lambda_{jj}}{2} \tag{5}$$

where the ij subscript refers to cross-interactions and the subscripts ii and jj refer to same-site interactions.

3.2. Simulation set-up

Molecular dynamics simulations for this study are performed in the NVT ensemble (constant number of molecules, N, constant volume, V, and constant temperature, T) using GROMACS version 2018 [**?**]. Each simulation uses the Velocity Verlet integrator with a 2 fs time-step, 1.4 nm cut-off for non-bonded interactions with tail corrections for energy and pressure [**?**], Nosé-Hoover thermostat with a time constant of 1 ps, and fixed bond-lengths constrained using LINCS with a LINCS-order of eight. Coulombic interactions are not computed as none of the force fields require partial charges for the compounds studied. The equilibration time is 0.1 ns for ethane and propane, 0.2 ns for n-butane, and 0.5 ns for all other compounds. The production time is 1 ns for ethane, 2 ns for propane and n-butane, and 4 ns for all other compounds. Replicate simulations are performed for n-octane to validate that a single MD run of this length agrees with the average of several replicates, to within the combined uncertainty. A system size of 400 molecules is used for ethane, propane, and n-butane, while all other compounds use 800 molecules. Example input files are provided as Supporting Information.

1. Two types of simulations performed, saturation and 293 K for compressed systems
2. Saturation simulations use the REFPROP densities such that, in some cases, the force field is actually in a metastable state
3. Performed some simulations at reported saturation conditions
4. NPT performed for each replicate such that a distribution of box sizes is obtained

5. Depending on the system, a simulation of 1, 2, 4, or 8 ns was used for the production stage
6. Details are in supporting information

3.3. Data analysis

Refer to Best Practices document

1. Use 40% sigma for cut-off
2. Fit sigma to power model
3. Fit viscosity to double exponential
4. Bootstrap uncertainties by resampling replicate simulations
5. 12 time origins

We have tried to

4. Results

Four normal and four branched alkanes of varying chain-length and degree of branching are simulated in this study. Specifically, we simulate ethane, propane, *n*-butane, *n*-octane, *n*-dodecane, *n*-hexadecane, 2-methylpropane, 2-methylbutane, 2-methylpentane, 3-methylpentane, 2,2-dimethylpropane, 2,3-dimethylbutane, and 2,2,4-trimethylpentane. These compounds were chosen to represent a diverse set of the normal and branched alkanes available in REFPROP [**? ? ? ? ? ? ? ?**]. Each compound was simulated using the TraPPE (UA LJ 12-6) and Potoff S/L (UA Mie 16-6) force fields. However, only 2-methylpropane and 2,3-dimethylpropane were simulated with AUA4 (AUA LJ 12-6) while 2,3-dimethylpropane and 2,2,4-trimethylpentane were not simulated using the TAMie (AUA Mie 14-6) force field.

4.1. Saturated Liquid

4.1.1. n-Alkanes

Figure 3 compares the TraPPE (UA LJ 12-6), Potoff (UA Mie 16-6), and TAMie (AUA Mie 14-6) saturated liquid viscosities for propane, *n*-butane, and *n*-octane. Similar to what

has been demonstrated in previous studies, the TraPPE force field significantly under predicts η^{sat} (between 30 and 80 %) with the deviation increasing towards the triple point temperature. By contrast, the Potoff and TAMie force fields agree with the REFPROP values for these compounds to within 10 % over the entire temperature range studied (which includes the triple point for propane), and do not demonstrate a strong temperature dependence.

Figure 4 compares the TraPPE, Potoff, and TAMie saturated liquid viscosities for *n*-dodecane and *n*-hexadecane. Although the TAMie and TraPPE results for these compounds are similar to those observed in Figure 3, it is quite surprising that the Potoff results are nearly identical to the TraPPE results (which significantly under predict η^{sat}).

4.1.2. Branched alkanes

Figures 5 and 6 compare the saturated liquid viscosities for each force field and branched alkane studied. Figures 5 and 6 present results for the compounds classified by Potoff as "short" and "long", respectively. Specifically, Figure 5 depicts 2-methylpropane, 2,2-dimethylpropane, 2-methylbutane, and 2,3-dimethylbutane, while Figure 6 contains 2-methylpentane, 3-methylpentane, and 2,2,4-trimethylpentane. Each compound was simulated using the TraPPE (UA LJ 12-6) and Potoff (UA Mie 16-6) force fields. However, only 2-methylpropane and 2,2-dimethylpropane were simulated with AUA4 (AUA LJ 12-6) while 2,2-dimethylpropane and 2,2,4-trimethylpentane were not simulated using the TAMie (AUA Mie 14-6) force field.

From Figures 5 and 6, we see that the Potoff S/L and TAMie force fields are not as accurate for these branched alkanes as for the normal alkanes. In particular, Potoff and TAMie demonstrates the same temperature dependence observed for other force fields, where the deviations are largest at lower temperatures. However, Potoff still provides considerable improvement compared to the LJ 12-6 based models, i.e., TraPPE and AUA4. Note that the performance is similar for the Potoff "short" and "long" parameters in Figures 5 and 6, respectively.

The deviations for each force field are largest for 2-methylpropane and 2,2-dimethylpropane. Since these compounds are primarily composed of CH_3 UA sites, this poor performance is likely due to the assumption that the CH_3 non-bonded parameters are transferable from

n-alkanes to branched alkanes. Improvement might be possible if the CH_3 parameters were different depending on the neighboring UA site type.

4.2. High pressure fluid

Section 4.1 demonstrated that Mie n-6 based force fields (Potoff and TAMie) are considerably more reliable for predicting saturated liquid viscosities than LJ 12-6 based force fields (TraPPE and AUA4). However, both the Potoff and TAMie non-bonded potentials use $n > 12$. Reference BLANK demonstrates that $n > 12$ leads to strong negative consequences at high densities/pressures. Specifically, $n > 12$ is too repulsive at short distances which leads to over estimates of pressure at high densities. For this reason, this section compares the different force fields above saturation pressure.

4.2.1. n-Alkanes

1. Propane has accurate viscosity-P but not viscosity-rho
2. Butane appears to agree more closely with recent REFPROP correlation

Figures 7, 8, and 9 compare the elevated pressure viscosities for propane, n-butane, and n-octane, respectively. Each compound is simulated using the TraPPE, Potoff, and TAMie force fields. Note that for propane and n-butane (Figures 7 and 8) each force field is simulated at the same density, while for n-octane (Figure 9) the force fields are simulated at the same pressure.

Figure 7 demonstrates that the TraPPE force field has a constant negative bias even with increasing density/pressure. The TAMie force field has the most accurate η-ρ dependence, i.e., the error does not increase with respect to density. By contrast, the Potoff potential demonstrates considerable over estimation of η at high densities, which is likely attributed to the overly repulsive Mie 16-6 potential at close distances. Remarkably, the Potoff force field is the most accurate at predicting the η-P dependence. This can be explained as a cancellation of errors since the Potoff force field significantly over predicts both viscosity and pressure at high densities.

The results in Figures 8 and 9 for n-butane and n-octane, respectively, are similar to those in Figure 7 for propane. Specifically, the TraPPE force field under predicts η at all densities/pressures, the TAMie force field provides the most accurate η-ρ dependence, while the Potoff force field over predicts η-ρ dependence but accurately predicts the η-P dependence.

4.2.2. Branched alkanes

1. Similar to n-alkanes?
2. Wrong torsions matters?

5. Discussion/Limitations

1. Discussion
   (a) Mie potentials parameterized with VLE data provide significant improvement over LJ 12-6
   (b) Potoff over-predicts $\eta - \rho$ dependence while TAMie is fairly accurate
   (c) Potoff appears to be slightly more accurate for $\eta - P$
   (d) Branched alkanes are not as accurate, perhaps assumption of transferability or torsional parameters
2. Limitations
   (a) Largest viscosity simulations are slow to converge and unclear if simulations are sufficiently long
   (b) Tail-corrections could impact dynamics
   (c) Using REFPROP saturation conditions instead of force fields

6. Conclusions

Acknowledgments

We are grateful for the internal review provided by NIST BERB Reviewer 1 and NIST BERB Reviewer 2 from the National Institute of Standards and Technology (NIST).

This research was performed while Richard A. Messerly held a National Research Council (NRC) Postdoctoral Research Associateship at NIST and while Michelle C. Anderson held a Summer Undergraduate Research Fellowship (SURF) position at NIST.

7. Supporting Information

7.1. Gromacs input files

1. Include all the .gro files
2. Include all the .top file templates
3. Include .mdp files
4. Or we can just include an example and then refer them to the GitHub website

7.2. Tabulated values

1. Ethane
   (a) Saturation
      i. Potoff
      ii. TraPPE
      iii. AUA4
      iv. TAMie
   (b) T293 highP
      i. Potoff
      ii. TraPPE
      iii. AUA4
      iv. TAMie
2. Propane
   (a) Saturation
      i. Potoff
      ii. TraPPE
      iii. AUA4

iv. TAMie

(b) T293 highP

i. Potoff

ii. TraPPE

iii. AUA4

iv. TAMie

3. n-Butane

(a) Saturation

i. Potoff

ii. TraPPE

iii. AUA4

iv. TAMie

(b) T293 highP

i. Potoff

ii. TraPPE

iii. AUA4

iv. TAMie

Repeat for all other compounds with corresponding potentials

7.3. Finite-size effects

1. Simulation results for 100, 200, 400, and 800 molecules

7.4. Simulation length effects

1. Verified that 1 ns is long enough for larger compounds

7.5. Validation Runs

1. Ethane NIST
2. n-Octane Literature

7.6. Bond types, Harmonic vs LINCS

1. Propane and n-butane with harmonic (arbirary bond constant) shows systematic increase

7.7. Green-Kubo analysis

1. Raw data, i.e., multiple replicates with the average
2. Exclude low time data and have a heurestic for determining the cut-off time

Example analysis, i.e., bootstrap distribution, replicates

7.8. MCMC?

Figure 2: Saturated liquid viscosities for ethane. Colors/symbols denote different force fields.

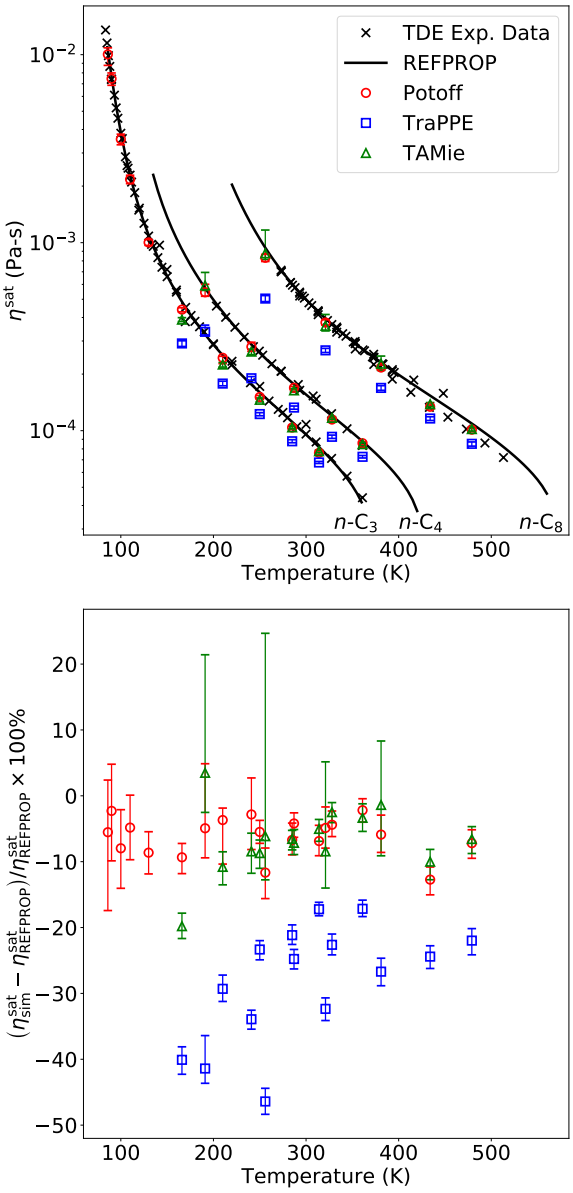

Figure 3: Saturated liquid viscosities for propane, n-butane, and n-octane. Colors/symbols denote different force fields.

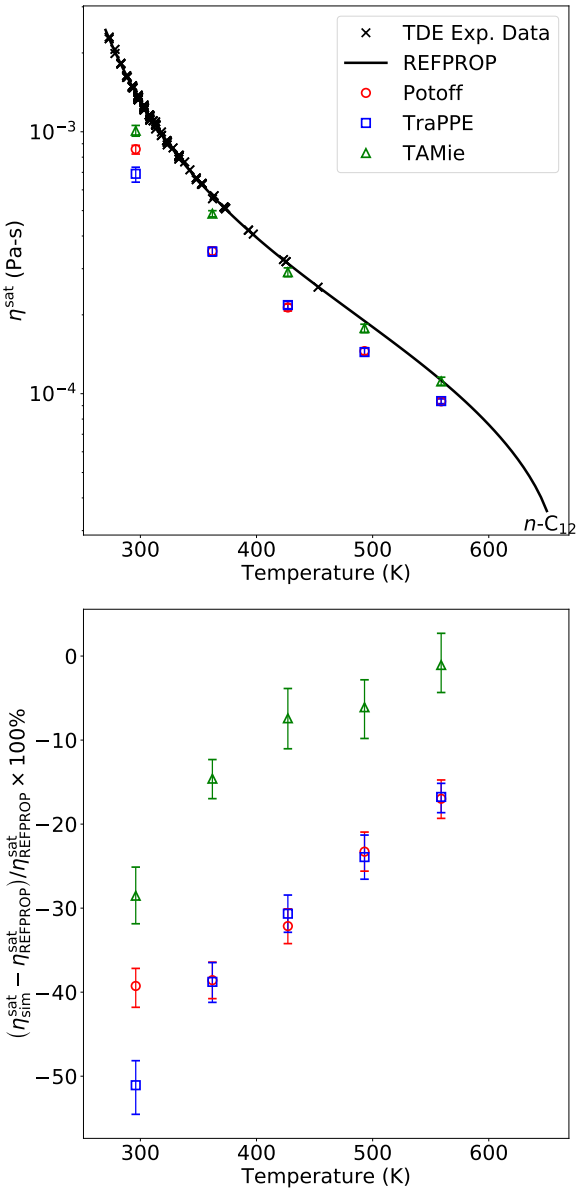

Figure 4: Saturated liquid viscosities for n-dodecane and n-hexadecane. Colors/symbols denote different force fields.

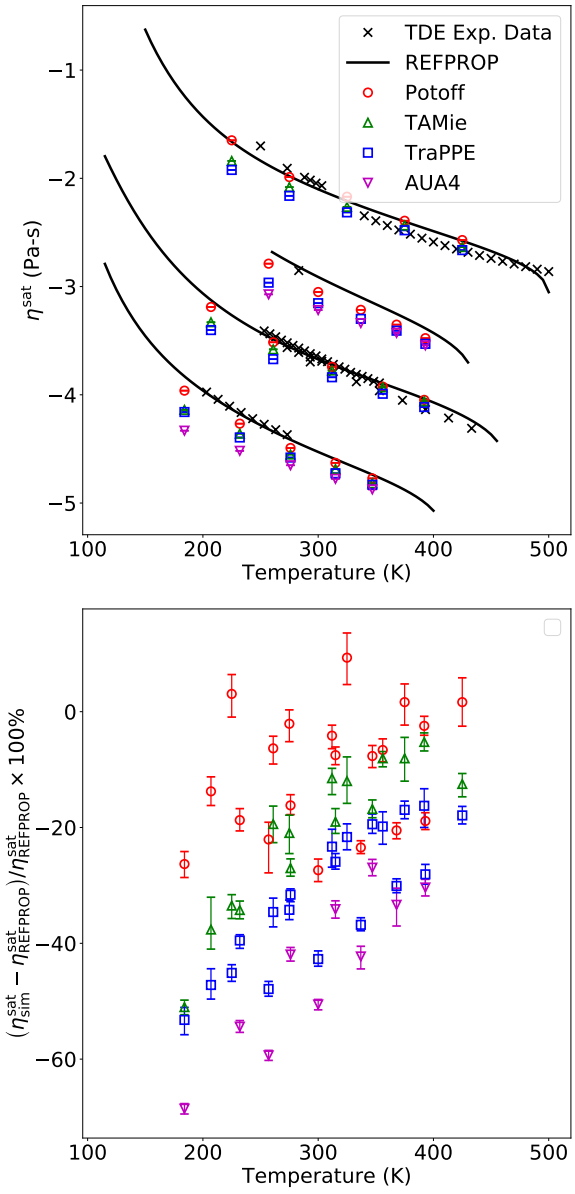

Figure 5: Saturated liquid viscosities for 2-methylpropane, 2,2-dimethylpropane, 2-methylbutane, and 2,3-dimethylbutane. Colors/symbols denote different force fields.

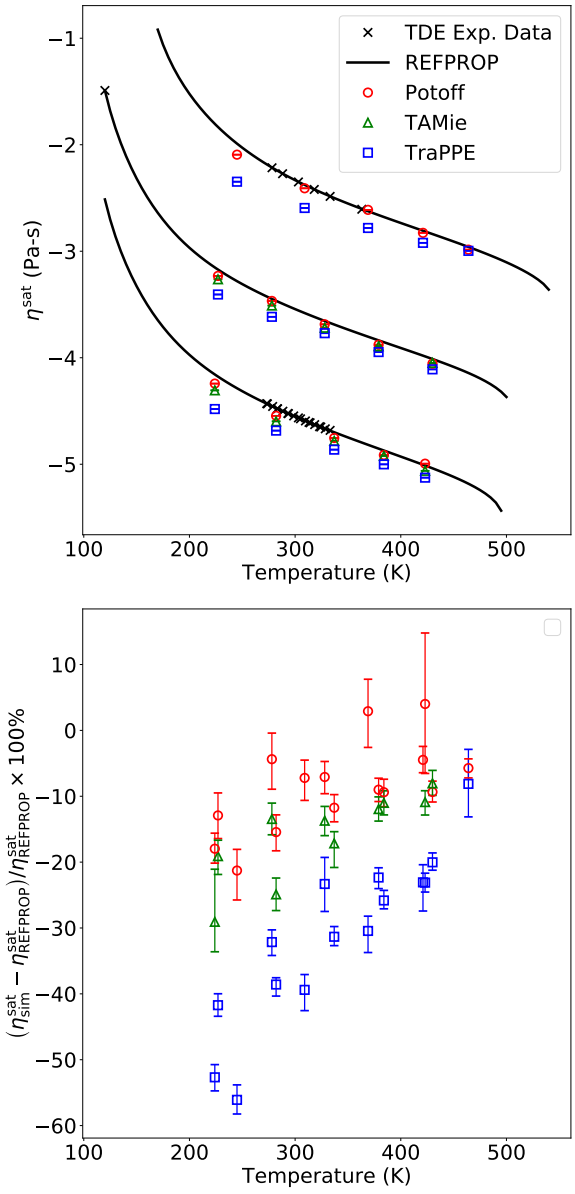

Figure 6: Saturated liquid viscosities for 2-methylpentane, 3-methylpentane, and 2,2,4-trimethylpentane. Colors/symbols denote different force fields.

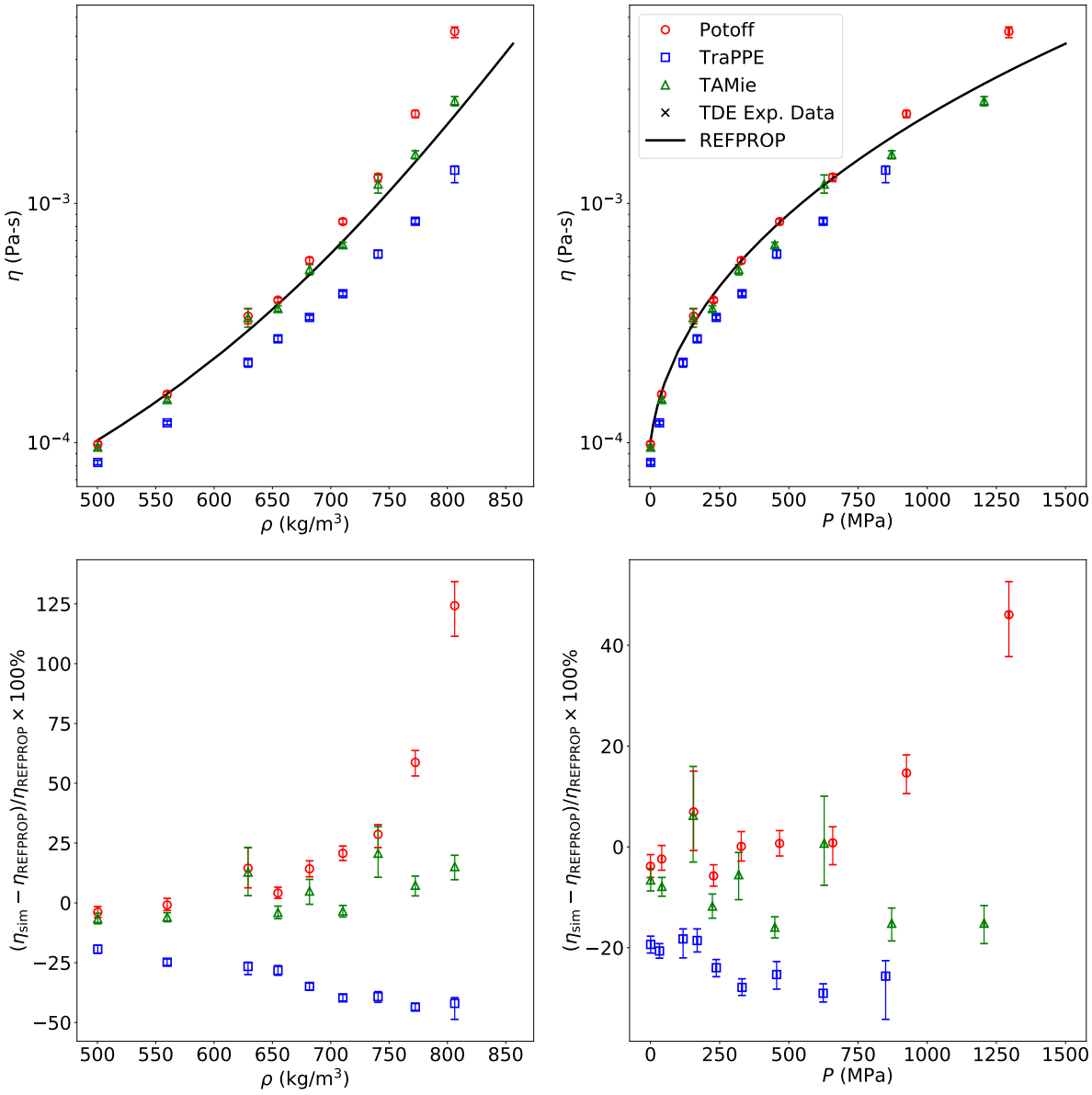

Figure 7: High density fluid viscosities at 293 K for propane. Colors/symbols denote different force fields.

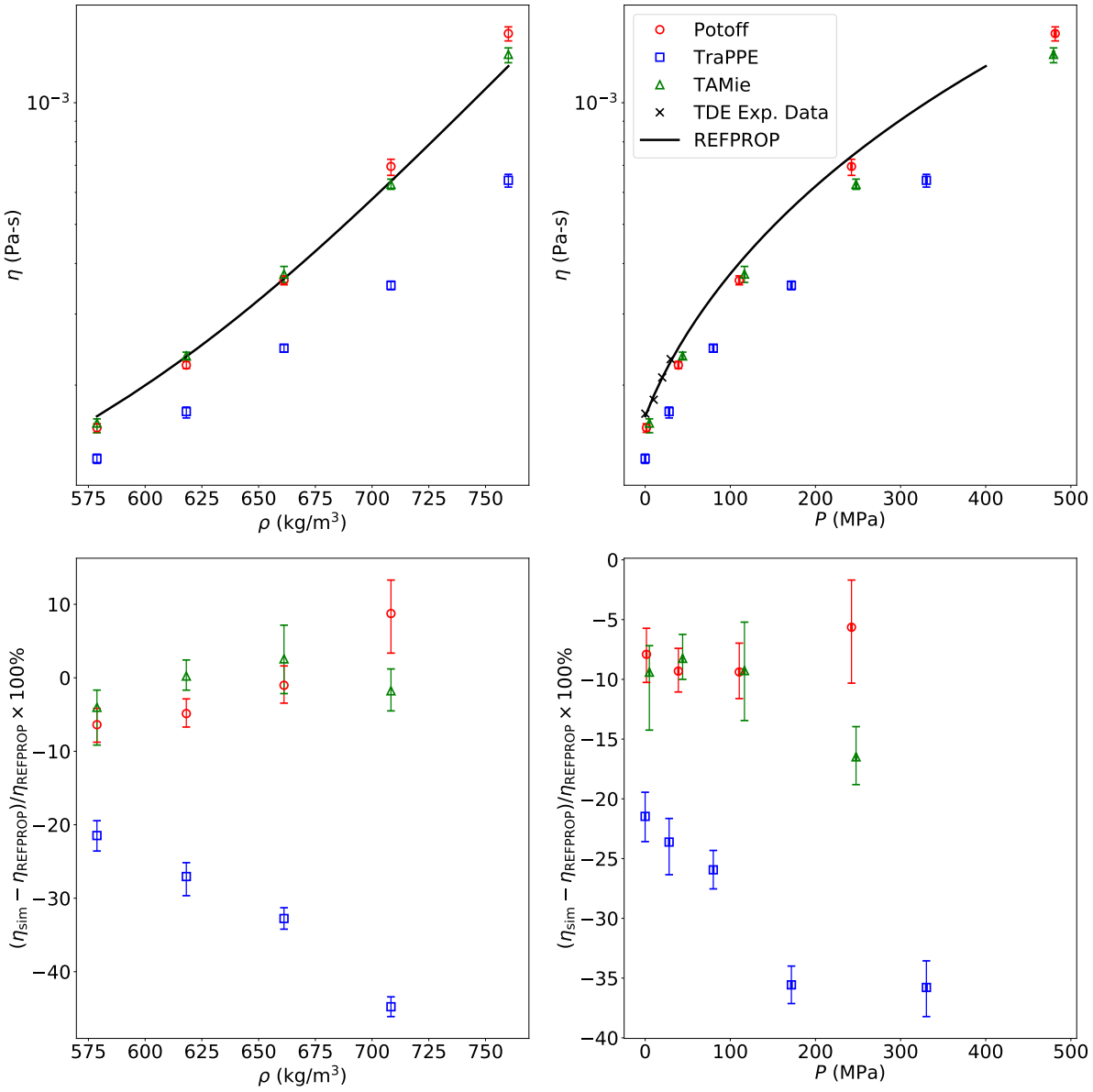

Figure 8: High density fluid viscosities at 293 K for n-butane. Colors/symbols denote different force fields.

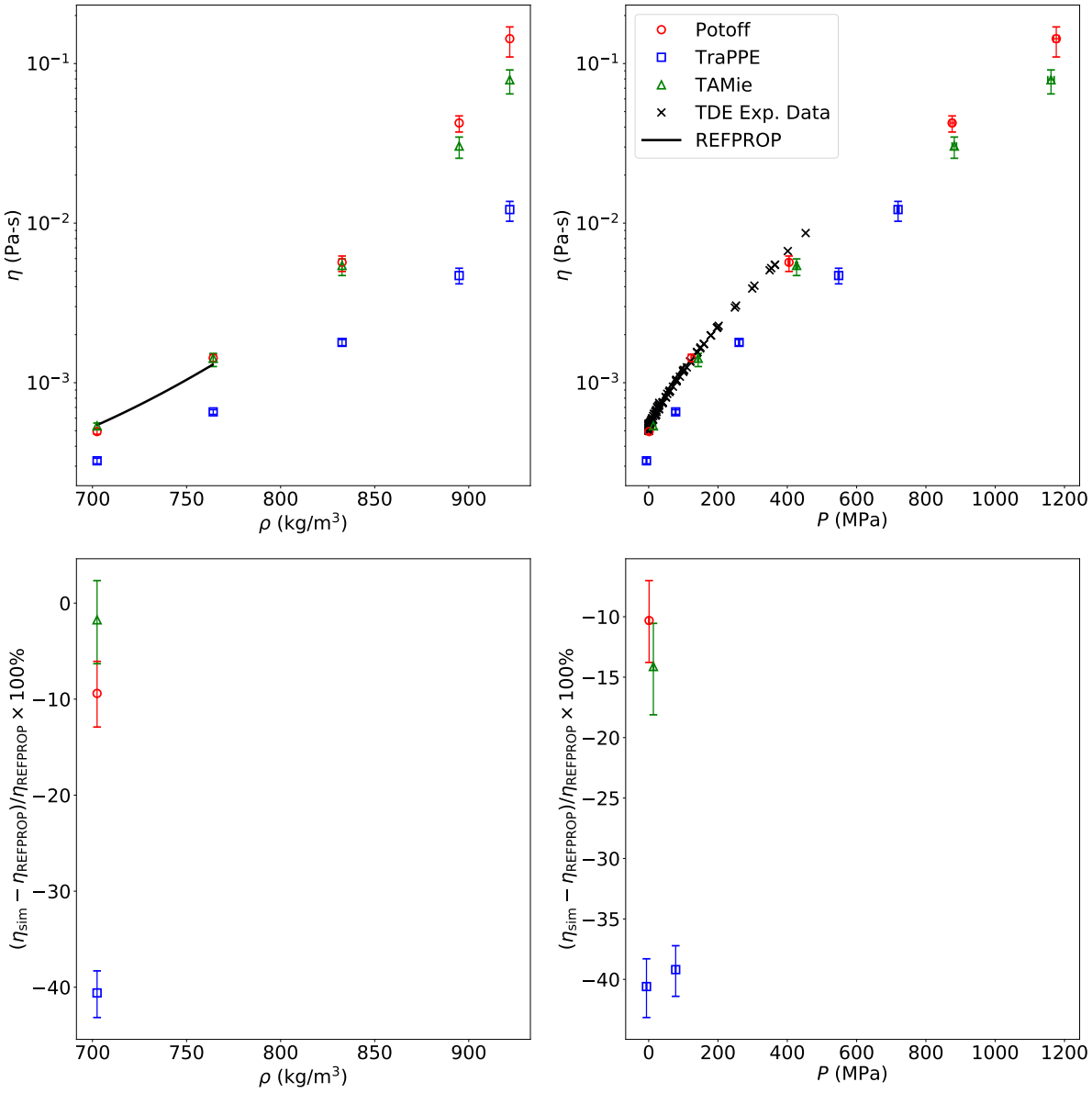

Figure 9: High density fluid viscosities at 293 K for n-octane. Colors/symbols denote different force fields.

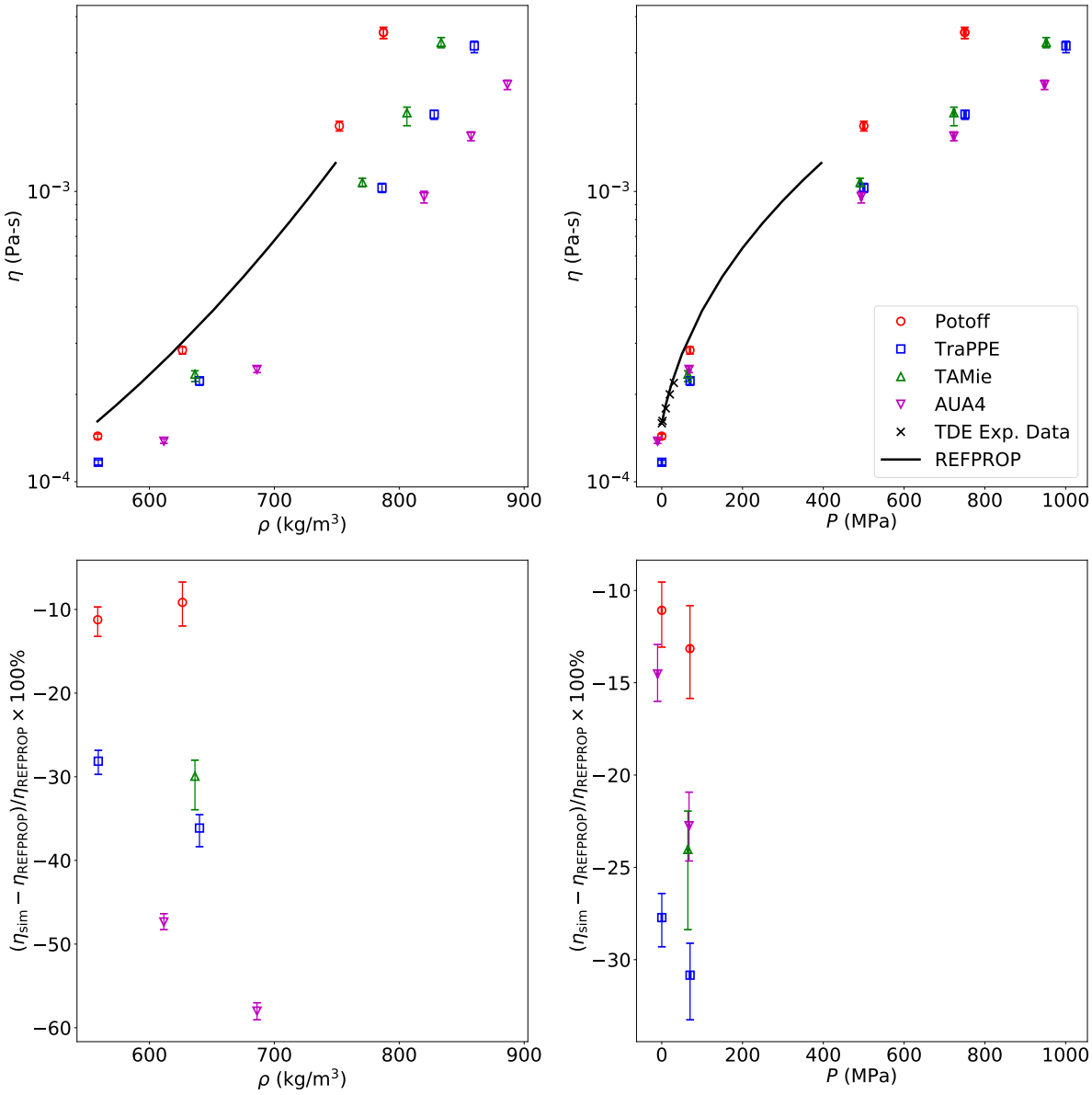

Figure 10: High density fluid viscosities at 293 K for 2-methylpropane. Colors/symbols denote different force fields.

Figure 11: High density fluid viscosities at 293 K for 2-methylbutane. Colors/symbols denote different force fields.

Figure 12: High density fluid viscosities at 293 K for 3-methylpentane. Colors/symbols denote different force fields.

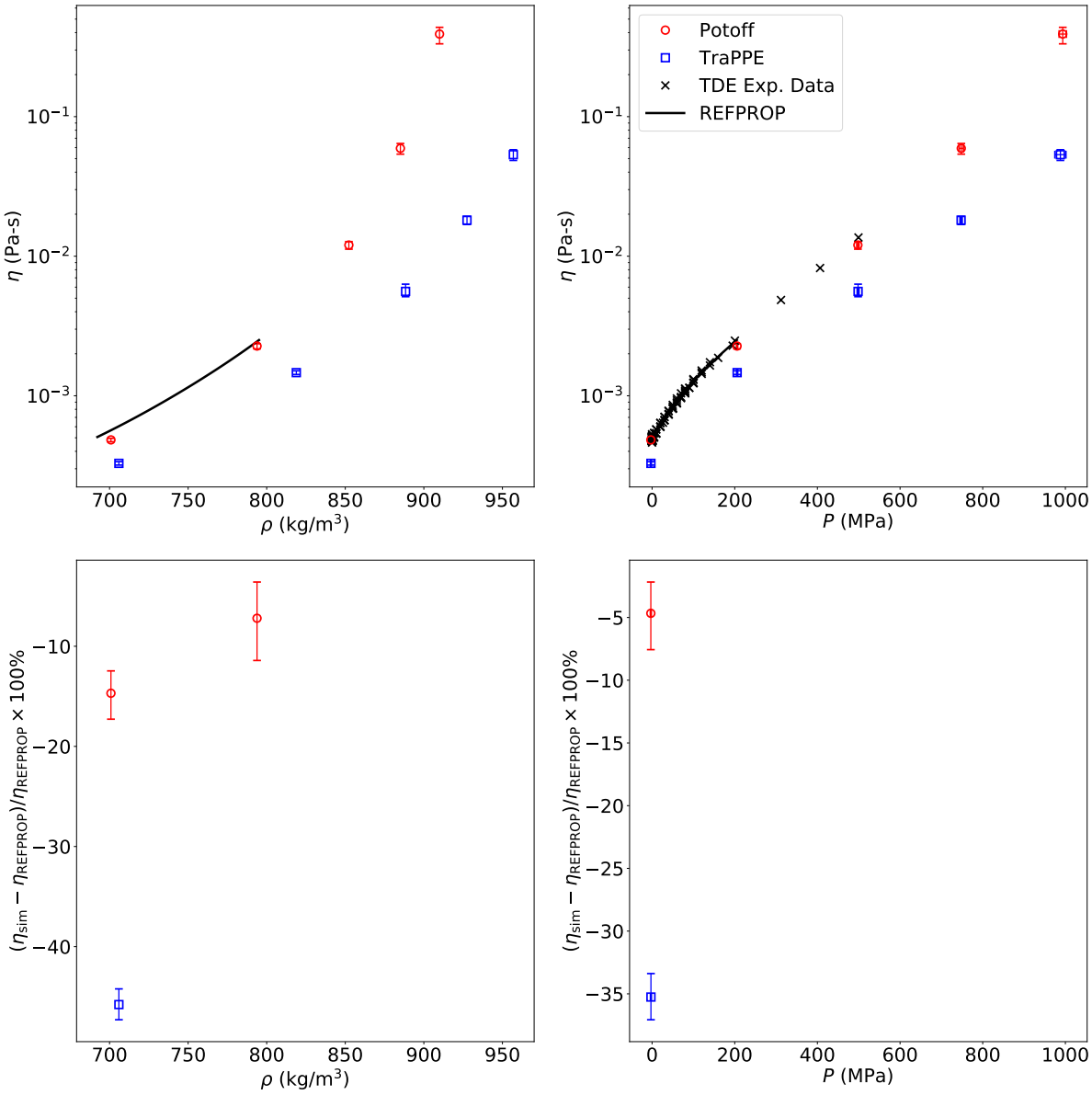

Figure 13: High density fluid viscosities at 293 K for 2,2,4-trimethylpentane. Colors/symbols denote different force fields.